Available online at www.sciencedirect.com
SCIENCE DIRECT®
Journal of Nuclear Materials 336 (2005) 1–10
journal of nuclear materials
www.elsevier.com/locate/jnucmat

Corrosion behaviors of US steels in flowing lead–bismuth eutectic (LBE)

Jinsuo Zhang [a,*], Ning Li [b], Yitung Chen [c], A.E. Rusanov [d]

[a] Decision and Application Division, and Center for Nonlinear Studies, Los Alamos National Laboratory, MS-K575, Los Alamos, NM 87544, USA
[b] Materials Science and Technology Division, Los Alamos National Laboratory, Los Alamos, NM 87544, USA
[c] Mechanical Department, The University of Nevada at Las Vegas, Las Vegas, NV 89154, USA
[d] Institute of Physics and Power Engineering, Obninsk, Russian Federation

Received 8 April 2004; accepted 10 August 2004

Abstract

Corrosion tests of several US martensitic and austenitic steels were performed in a forced circulation lead–bismuth eutectic non-isothermal loop at the Institute of Physics and Power Engineering (IPPE), Russia. Tube and rod specimens of austenitic steels 316/316L, D-9, and martensitic steels HT-9, T-410 were inserted in the loop. Experiments were carried out simultaneously at 460 °C and 550 °C for 1000, 2000 and 3000 h. The flow velocity at the test sections was 1.9 m/s and the oxygen concentration in LBE was in the range of 0.03–0.05 wppm. The results showed that at 460 °C, all the test steels have satisfactory corrosion resistance: a thin protective oxide layer formed on the steel surfaces and no observable dissolution of steel components occurred. At 550 °C, rod specimens suffered rather severe local liquid metal corrosion and slot corrosion; while tube specimens were subject to oxidation and formed double-layer oxide films that can be roughly described as a porous Fe_3O_4 outer layer over a chrome-rich spinel inner layer. Neglecting the mass transfer corrosion effects by the flowing LBE, calculations based on Wagner's theory reproduce the experimental results on the oxide thickness, indicating that the oxide growth mechanism of steels in LBE is similar to that of steels in air/steam, with slight modification by dissolution and oxide dissociation at the liquid metal interface.

1. Introduction

Lead-alloys (lead, lead–bismuth eutectic) have emerged as strong candidates for applications in advanced reactors and transmutation systems as nuclear coolants and high-power spallation neutron targets. However, it is widely recognized that corrosion of materials by lead-alloys presents a critical barrier to their industrial uses. R&D projects have been set up to study the corrosion in test facilities and develop mitigation techniques and materials.

One of the central techniques under development in lead-alloy coolant technology is the active oxygen control technique to build up and maintain protective oxide films. Several experimental studies addressing the corrosion and oxidation issues in lead or lead–bismuth

* Corresponding author. Tel.: +1 505 667 7444; fax: +1 505 665 2897/2659.
E-mail address: jzhang@cnls.lanl.gov (J. Zhang).

0022-3115/$ - see front matter © 2004 Elsevier B.V. All rights reserved.
doi:10.1016/j.jnucmat.2004.08.002

systems have been published in the recent past [1–11]. These experiments show that the temperature, oxygen concentration, flow velocity, steel composition, etc. play important roles in the corrosion and oxidation processes. However, we cannot reach definitive conclusions or correlations between the corrosion and the hydraulic factors based on the existing experimental results because the results are scarce and the test conditions are scattered. At the present time, these test results cannot be easily interpreted and applied for general design purposes.

In this reported study, several US martensitic and austenitic steels were tested in a flowing LBE loop (CU-1M loop at IPPE) at 460 °C and 550 °C for up to 3000 h. The key experimental results are presented and discussed. Comparisons are made with experimental results on other steels having similar compositions, revealing several types of corrosion behaviors of US steels in flowing LBE. The present results add to the available databases.

The experiments reported here and the post-test analyses were performed at IPPE under the LANL contract of #H 12030008-35 [12].

2. Corrosion test

The corrosion tests were performed in the experimental facility of IPPE. The loop is a non-isothermal forced-circulation loop with 60 L of LBE and a flow capacity of 5 m^3/h. For the present experiments, the highest and lowest temperatures in the loop are 600 °C and 300 °C, respectively.

Three types of austenitic steel (316, 316L, D-9) and two types of martensitic steel (T-410, HT-9) were tested. The chemical compositions of the steels are listed in Table 1. Samples are ∅8 mm rods made of 316L and T-410 steels, ∅8 × 1 mm tube made of 316 steel, and ∅6 × 0.3 tubes made of D-9 and HT-9 steels. All specimens are 160 mm long. For the tube specimens, only the outer surfaces are exposed to flowing LBE. The D-9 and HT-9 specimens were cut from EBR-II driver fuel cladding stock from the Argonne National Laboratory [13]. All specimens were put into the test loop without additional surface preparations. During the experiment, the Russian ferritic–martensitic steel EP823 steel (∅8 and ∅6) were also tested. But we will not report the results on such steel in the present article. The arrangement of the specimens in the test section is shown in Fig. 1.

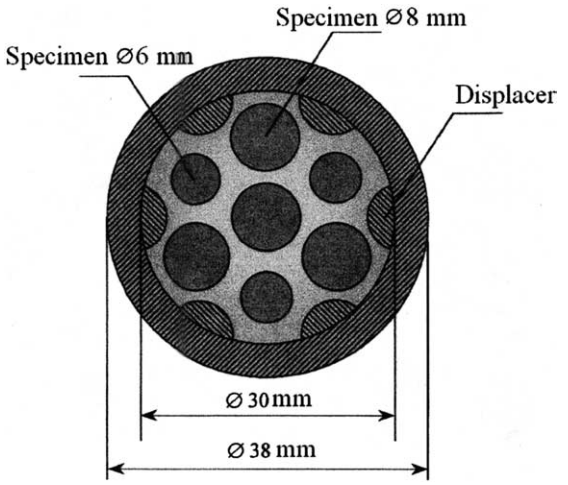

Fig. 1. Cross-section of the test section.

Experiments were carried out simultaneously at 460 °C and 550 °C. The flow velocity at the test sections was 1.9 m/s and the oxygen concentration in LBE was in the range of 0.03–0.05 wppm. After 1000 h of tests, half of the specimens were extracted and replaced with fresh specimens. The test then continued for another 2000 h. Therefore we have three sets of specimens for 1000, 2000 and 3000 h of tests. After testing, specimens were extracted and residual LBE were cleaned by washing the samples in hot glycerin in the temperature range of 150–180 °C. Weight change measurement, optical microscopy, SEM and X-Ray analysis were performed afterwards.

3. Results

3.1. Weight changes

The weight changes of the steel samples after the corrosion tests provide direct information about the gross

Table 1
Chemical composition of steels used in the corrosion tests (wt%)

Steel	C	Si	Ni	Mn	Cr	Mo	Other
316	<0.08	<1.0	10–14	<2.0	16–18	2.0	–
316L	<0.03	<1.0	10–14	<2.0	16–18	2.0	–
D-9	0.04	0.85	13.6	2.1	13.6	1.67	0.30Ti
HT-9	0.22	1.0	0.59	0.58	12.0	1.11	0.50W
T-410	–	0.30	0.34	1.0	12.5	–	–

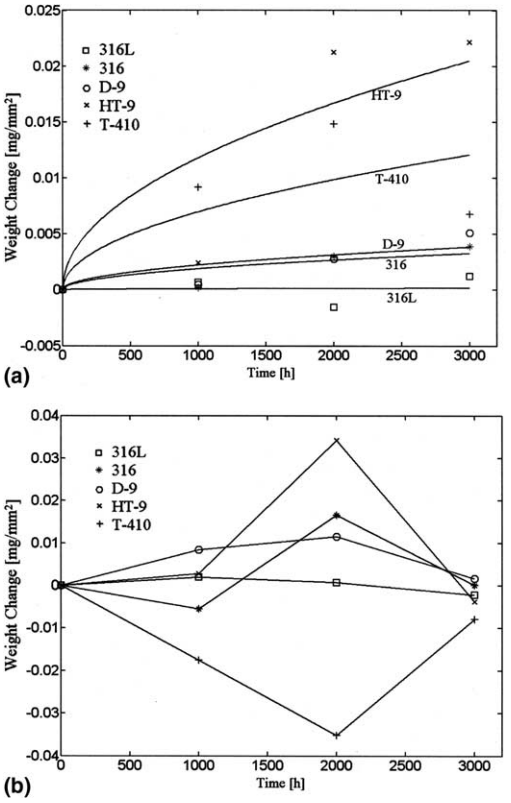

Fig. 2. Specific weight changes of the steels tested in the CU-1M LBE loop. (a) $T = 460\,^{\circ}C$; (b) $T = 550\,^{\circ}C$.

corrosion and oxidation effect. Fig. 2 shows the specific weight changes over time for all the samples at 460 °C and 550 °C.

Fig. 2(a) indicates that weights of all steel samples tested at 460 °C increase with time, except for that of the 316L sample after 2000 h of tests. The weight gain is due to the oxidation reaction, while the weight loss of 316L samples is due to slot corrosion. The weigh increases of martensitic steels (HT-9 and T-410) are much higher than those of austenitic steels (316L/316 and D-9). Results were fitted with a parabolic law and the parabolic trends in the experimental data can be readily observed.

The weight changes of all the steel samples tested at 550 °C are more complicated than those of samples tested at 460 °C (Fig. 2(b)). Weight losses are observed for samples made of 316L, 316 and T-410. For the samples made of D-9 and HT-9, the characteristics of the weight change in the first 2000 h testing period are different from those in the testing period after 2000 h. During the first 2000 h, the weight increases with time, while after 2000 h of tests, the weight decreases.

3.2. Examination of the solid/liquid interface

3.2.1. Austenitic steels (316, 3161, D-9)

At 460 °C, a very thin oxide layer formed on the surface of the tube specimen made of 316 steel after 1000, 2000 and 3000 h of tests. The oxide layer thickness is about <1 μm, 2–4 μm and 2–6 μm after 1000, 2000 and 3000 h, respectively. The oxide layer (Fig. 3(a)) is non-uniform and is composed of Fe–Cr spinel Me_3O_4 (Me = Fe, Cr). No corrosion damage by dissolution of steel components into the liquid metal (liquid metal corrosion) was detected, indicating that the thin oxide layer can protect the steel from direct dissolution. At 550 °C, the oxide layer has a double-layer structure (Fig. 3(b)) with the outer layer less compact than the inter layer. The loose outer layer is mainly composed of magnetite (Fe_3O_4) and the compact inner layer is mainly composed of Fe–Cr spinel. The duplex oxide layer thickness is 4–10 μm, 16–20 μm and 10–32 μm after testing 1000, 2000 and 3000 h, respectively, much larger than that at 460 °C.

Although the 316L steel has almost the same chemical composition with 316 steel (Table 1), the rod specimen made of 316L steel exhibited very different corrosion behaviors from the tube specimens made of 316 steel. At the lower temperature (460 °C), the oxide thickness is less than 1 μm after testing for 1000 and 2000 h. Only very thin oxide films (~1 μm) were detected at some locations on the steel surface after 3000 h. Slot corrosion (Fig. 4) was detected on the steel surface after

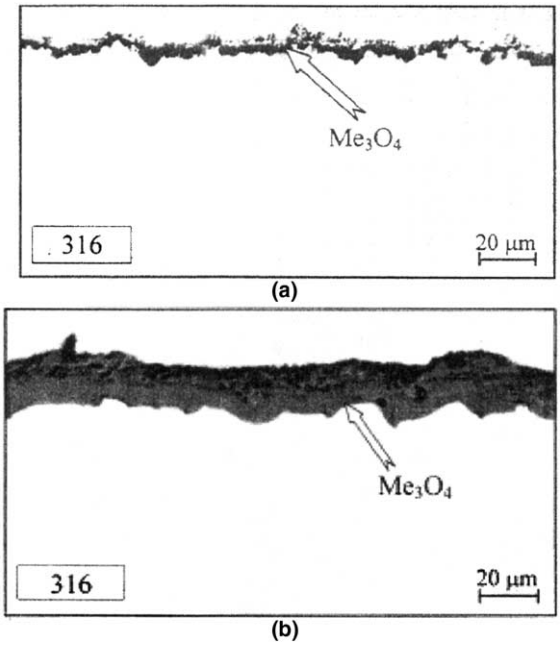

Fig. 3. Cross-section of 316 (tube) after exposed to flowing LBE for 2000. (a) $T = 460\,^{\circ}C$; (b) $T = 550\,^{\circ}C$.

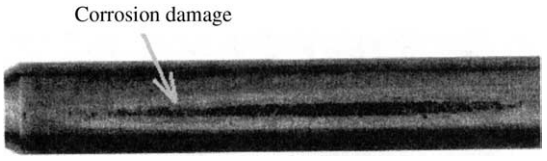

Fig. 4. Slot corrosion of 316L steel at 460 °C for 2000 h.

2000 h of tests. The depth of the corrode layer is about 60 μm and its length is about 40 mm.

At 550 °C, the oxide layer still has a single-layer structure. After 2000 h of tests, only small pieces of oxide film with ~1 μm thickness were detected, and after 3000 h of tests, 1–4 μm thick pieces of oxide films on the steel surface could be detected. Local oxide thickness can reach 4–12 μm after 2000 h and 10 μm after 3000 h. Except for the small pieces of oxide films, liquid metal corrosion was observed at the end of the rod specimen after 2000 h and the damaged depth was about 160 μm. The microstructure in the corrosion damaged area after 3000 h is shown in Fig. 5. Both liquid metal corrosion and slot corrosion were observed. The depth and length (along the axis) of the slot corrosion are 120–140 μm and 820 μm, respectively. Local liquid metal corrosion depth could reach a value of 220 μm.

The cross-section views of the tube specimen made of D-9 steel for testing duration of 2000 h at 550 °C are shown in Fig. 6. For this steel, no corrosion damage was observed at the present operating conditions. After 1000 h of tests at 460 °C, it was impossible to observe the oxide film on the steel surface by the metallographic method (the oxide layer is <1 μm). The oxide thickness becomes thicker in time. The thickness reaches within 4–6 μm after 2000 h and some islets of film have thickness within 2–6 μm after 3000 h of tests. At 550 °C, a double-layer film with thickness of 20–36 μm formed on D-9 steel surface after 2000 h of testing, similar to the oxide formed on the 316 steel. After 3000 h of tests,

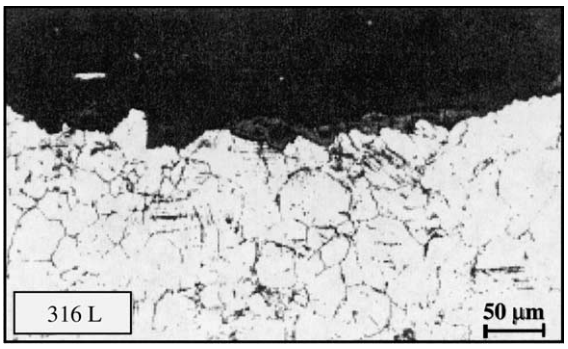

Fig. 5. The microstructure of 316L steel in the corrosion damaged area at 550 °C after 3000 h.

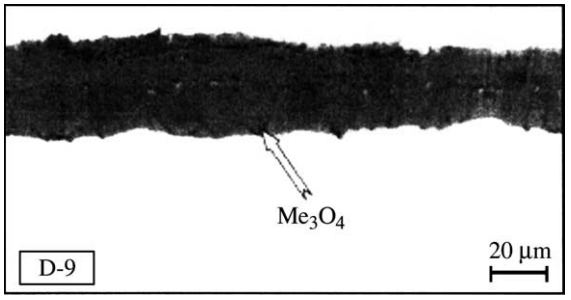

Fig. 6. Cross-section of D-9 (tube) after exposure in flowing LBE for 2000 h at $T = 550$ °C.

in some areas, maximum film thickness is 40 μm. No typical liquid metal corrosion was detected.

Distributions of Fe, Cr and Ni in the oxide layer are also measured. For D-9 and 316 steels (tube specimens), there is an enrichment of Cr in the inner oxide layer where the iron concentration is at a minimum. The outer oxide layer contains more iron than that in the inner oxide layer. The ratio of the outer layer to the inner layer is around 1:1. The oxide layer of 316L (rod) steel is very thin, in which Cr is enriched. For these austenitic steels, nickel is enriched near the steel/oxide interface, indicating that Ni diffuses inward in the steel during oxide layer formation.

3.2.2. Marstensitic steels (HT-9, T-410)

No liquid metal corrosion occurred and a double-layer oxide film formed on the steel surface of HT-9 (tube specimen) at 460 and 550 °C up to 3000 h (Fig. 7). The thickness increases with time and temperature. At 460 °C, the film thickness is 1–8, 12–14 and 14–16 μm after 1000, 2000 and 3000 h of tests, respectively. At 550 °C after 1000 h of tests, a smooth oxide film with thickness up to 8 μm formed. The thickness increases to within 32–36 μm after 2000 h, and, the thickness reaches an average of 38 μm with some patches reaching 44 μm after 3000 h. An oxygen diffusion layer underneath the oxide layer after 3000 h of exposure at 550 °C was observed (Fig. 7(b)). The inner Cr-rich spinel layer is slightly thicker than the outer layer where Fe is rich.

Cross-section views of T-410 are shown in Fig. 8 after 3000 h of tests at 460 (Fig. 8(a)) and 550 °C (Fig. 8(b)). At 460 °C, the oxide film has no double-layer structure and is not uniform. Most of the oxide layer is composed of the Cr-rich spinel. After 1000 h of tests, the thickness is in the range of 1–12 μm, and after 2000 and 3000 h of tests, the thickness is in the ranges of 12–14 and 4–20 μm, respectively. But in some areas, the thickness is less than 1 μm. At 550 °C, the double-layer structure of the oxide film was not clearly observed even after 3000 h of tests (Fig. 8(b)) and the single-layer structure persists. The thickness of the discontinuous oxide film

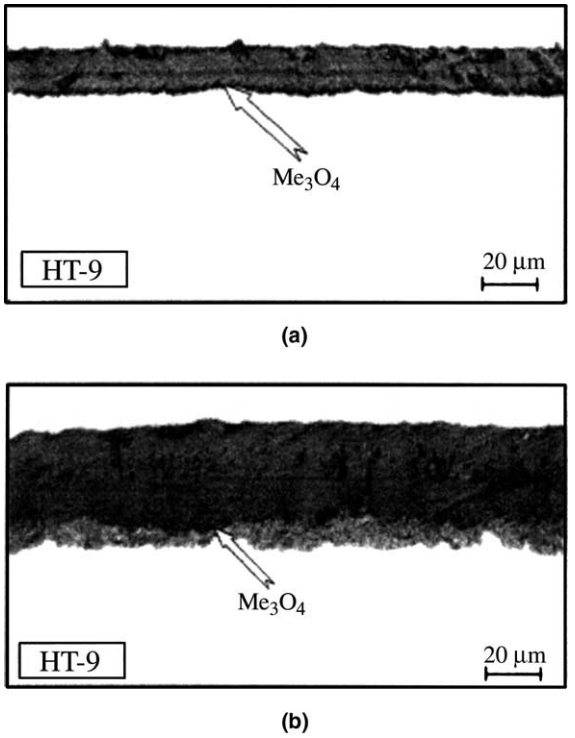

Fig. 7. Cross-section views of HT-9 (tube) after 2000 and 3000 h of tests in flowing LBE: (a) after 2000 h of tests at $T = 460\,^{\circ}C$; (b) after 3000 h of tests at $T = 550\,^{\circ}C$.

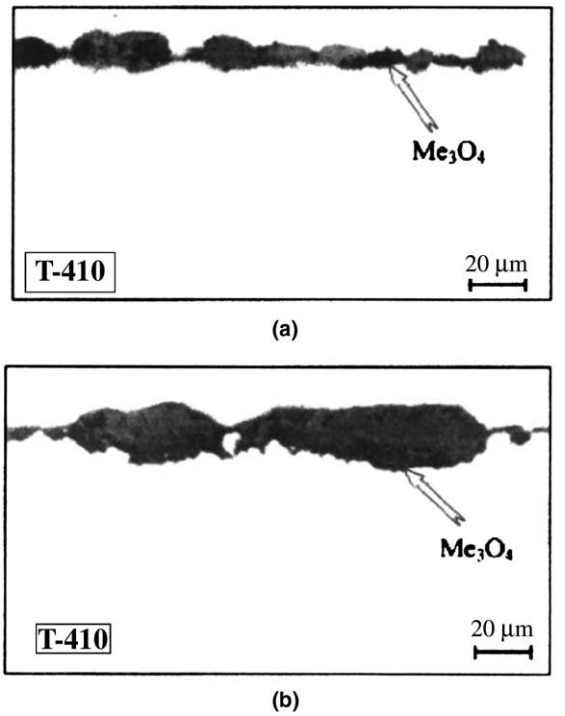

Fig. 8. Cross-section of T-410 (rod) after exposure in flowing LBE for 3000 h at 460 and 550 °C: (a) $T = 460\,^{\circ}C$; (b) $T = 450\,^{\circ}C$.

on the surface is 1–30, 1–50 and 4–36 μm after 1000, 2000 and 3000 h of tests, respectively.

Along with oxidation, the rod specimen of T-410 steel was subjected to heavy liquid metal corrosion. Even at the lower temperature (460 °C), local damage was observed after 2000 and 3000 h of tests. Depth of the damage could reach 100 μm. At 550 °C, liquid metal corrosion occurred after 1000 h. The corrosion depth is 220, 150–170, and ~300 μm after 1000, 2000 and 3000 h of tests. Except for the liquid metal corrosion, slot corrosion was revealed after 3000 h at 550 °C. The length and the depth of the slot corrosion are about 60 mm and 80 μm, respectively.

Similar to the austenitic steels, the Ni concentration near the oxide/steel interface was enhanced for both HT-9 and T-410.

4. Discussions

4.1. Oxide compositions

Experimental results in air indicate that the compositions of oxide formed on Fe–Cr alloy surfaces depend strongly on Cr content. It appears that a minimum of approximately 18 wt% Cr is needed to develop a continuous Cr_2O_3 scales against further oxidation attack [14]. Accordingly, it is unlikely to form pure Cr oxide films in the present experiments because Cr fraction in all the selected US steels is less than 18 wt%.

At 460 °C, specimens of austenitic steels (D-9, 316L and 316) with higher Cr content than martensitic steels (HT-9 and T-410) had single-layer spinel oxide films up to 3000 h of tests. At 550 °C, double-layer oxide films formed on tube specimens made of 316 and D-9 steels, while only single-layer oxide film formed on rod specimens made of 316L.

The nickel content was enhanced near the oxide/steel interface for all the austenitic steels. No ferritic layer characterized by preferential nickel dissolution was observed even at 550 °C up to 3000 h, indicating that the oxide layer can prevent nickel dissolution into LBE. The phenomena are consistent with previous experimental results of 316L steel at temperature 300 and 470 °C in flowing LBE with an oxygen concentration of 0.01 wppm [1].

At 460 °C, the single-layer oxide films can protect the steel from direct dissolution. At 550 °C, heavy dissolution corrosion damages were observed for rod specimens made of 316L on which only single-layer oxide film

formed, showing that the single-layer oxide film cannot protect the materials at this higher temperature. No liquid metal corrosion was observed for the tube specimens with formation of double-layer oxide films.

The 316 and 316L steels have almost the same chemical compositions, except for a small difference in the carbon concentration (Table 1). However, the specimens made of 316 and 316L steels exhibited very different behaviors at 550 °C under the present experimental conditions: the tube specimens (316 steel) were subjected to oxidation and thick double-layer oxide films formed, while the rod specimens (316L samples) were subjected to dissolution and only very thin single-layer oxide films formed in some areas.

Muller et al. [7] studied the 316L steel behaviors at 420, 550 and 600 °C in flowing LBE with an oxygen concentration of 0.01 ppm and a flow velocity of 2 m/s after 2000 h of tests. It was reported that there was a thin oxide film at 420 °C which was similar to the present result at 460 °C. At 550 °C, the authors found a double-layer oxide film on the 316L specimen surface, which is very different from the present results for 316L steel, but similar to the present results for 316 steel. Therefore, the different carbon concentrations in 316L and 316 steels is not the main reason that lead to the significantly different oxidation behaviors of the two steels. At 600 °C, Muller et al. observed deep liquid metal penetration and massive ablation of materials by erosion.

Experiments in static LBE with saturated oxygen [6] showed that the thin protective oxide layer could form on 316L steel surface at 300 and 400 °C, while dissolution corrosion occurred at 550 °C and in few areas a thin oxide was found similar to the present experimental results of 316L steel in flowing LBE. Other experimental results on 316L steel in CU-1 [3] indicate that the steel has a satisfying resistance to corrosion even for low oxygen contents (0.001–0.0001 ppm) at 470 °C and is subjected to dissolution corrosion even at a higher oxygen content (0.01 ppm) at 600 °C. In JLBL-1 loop [15] where oxygen was not actively controlled and likely at very low concentrations, experimental results on 316 steel indicated that the steel was subjected to dissolution at 450 °C and no oxide film was observed.

These experimental results of 316 and 316L steels are scattered. However we can make some general conclusions based on these results. First, a thin oxide layer can form on the steel surface if the temperature is lower than 500 °C and it can protect the steel against liquid metal corrosion (except for results in Ref. [15]). Second, if the temperature is 550 °C or higher, both thin oxide films and thick double-layer oxide films could form on 316/316L steels depending on the surface and experimental conditions. Third, the single-layer oxide film cannot prevent dissolution of some steel components at 550 °C or above, while the double-layer oxide film can protect the steel against direct dissolution.

The behaviors of HT-9 steel in flowing LBE under the present experimental conditions are consistent with the experimental results of other martensitic/ferritic steels, such as MANET steel [7], T91 steel [6,1]. Quite thin, compact double-layer oxide films formed on the steel surface at 460 °C. At 550 °C, the oxide film still has a double-layer structure, but the out layer was looser compared to that at 460 °C. For the T-410 steel, no significant duplex oxide film formed and heavy liquid metal corrosion was observed. At the present, it is difficult to interpret why the T-410 exhibits very different behaviors from the other martensitic steels. The reason may be that the cold-rolled process (the rod sample is made by cold-rolled process) resulted in small grain sizes or some other mechanical forces such as high surface shear stress by the flow removed the protective oxide layer.

The present studies show that the compact inner oxide layer is composed of $(Fe,Cr)_3O_4$ and the outer oxide layer is composed of Fe_3O_4. The inner oxide compositions are consistent with the experimental results from martensitic Optifer IVc and EP823 steels in LBE [1] and Fe–9%Cr alloy in air [16]. While Fazio et al. [5] reported that the inner oxide layer is composed of $Fe(Fe_{1-x}Cr_x)O_4$ for MANET and F82H steels. Another experiment on pre-oxidized F82H steel [17] indicates that the inner oxide layer is composed of $(Fe_{1-x}Cr_x)_2O_3$.

It was reported that the interface between the outer and inner oxide layers (magnetite/spinel) was smooth and coincided with the original steel surface for oxidation in gaseous environment [16] and steam [18]. The typical thickness ratio of the inner layer to the outer layer is between 1:1.1 (Ref. [18]) and 1:1.4 (Ref. [19]). Taylor et al. [16] reported that the ratio varied between 1:1.1 and 1.67. Because the thickness of the oxide film is not uniform in the present experiments, it is difficult to measure the ratio between the outer layer and the inner layer. The approximate average ratio is 1:1, which is slightly larger than that of steels in air and steam and consistent with scale removal in flowing LBE.

4.2. Oxidation mechanisms

The present tests of steels in flowing LBE cannot fully elucidate the mechanism of formation of oxide films of steels in LBE environments. For the single-layer oxide, it is reasonable to assume that the oxidation reaction occurs at the LBE/oxide interface, because the self-diffusion coefficient of oxygen through the spinel is much less than that of metals [20]. Therefore, the growth of the single-layer spinel oxide films on austenitic steel at 460 °C is due to the outward diffusion of the steel components (iron and chromium).

The mechanism of duplex oxide films formation is very complicated and not well understood at the present even in gaseous environments. Experimental results in air indicate that the diffusion coefficient of Cr is much

smaller than that of Fe in the spinel oxide film [21]. Therefore, especially for steels with low Cr content, the amount of Cr reaching the surface is not enough to form more spinel and iron oxide forms. The fact that Fe–Cr spinel-magnetite interface is situated at the original steel surface has led researchers to conclude that the growth of the outer magnetite layer occurs by migration of iron outwards and that the inner Fe–Cr spinel layer grows by oxidant movement through the scale [22]. It is the outer layer growth that controls the oxidation process and the inner spinel oxide takes up the space produced by the consumption of the original steel.

This mechanism has been verified by experiments using the sequential $^{16}O/^{18}O$ oxidation technique [16,23]. The experiments also showed that pure magnetite formation occurs at the gas/oxide interface, while the spinel oxide formation occurs throughout the inner layer. The open question is how oxygen gets to the inner layer with a very small self-diffusion coefficient.

There should be some fast paths for oxygen to arrive at the inner layer. Several fast paths for species transport in oxide scales were given in Ref. [24]: grain boundary diffusion, voids, porosities, microchannels, etc. However, some contradictions arise if the oxygen transport during the duplex oxide formation is through the aforementioned fast paths. Experimental results [25] indicate that diffusion of oxygen along grain boundaries is too slow to account for the inner layer growth. Voids are always observed in oxide films, but experimental investigations [26] conclude that the voids do not aggregate to pores traversing through the outer oxide layer. Although other experimental results [27] showed that the observed pores were probably continuous across the oxide layer, the corrosion model of Castle and Masterson [28] of steel in steam based on the assumption that the oxygen transported in pores can not account for the observed corrosion rate [29].

Although the present analysis showed the outer oxide films to be porous and much looser than the inner oxide films, no liquid metal penetrations were observed. This would exclude that the oxygen transport is due to the diffusion in the solution (LBE) that penetrates the oxide film through the pores. The oxygen diffusion mechanism(s) cannot be identified based on the existing results. For more comprehensive understanding of the scientific basis of LBE technology, further studies on the oxidation mechanisms in LBE (flowing and static) should be carried out.

4.3. Oxidation kinetics

Although the inward oxygen diffusion mechanism is not identified, it is known that the growth rate of the duplex film is determined by the outward transport of iron cations [25]. Assuming a parabolic growth law and taking into account the mass transfer corrosion at the LBE/oxide interface, the thickness of the outer layer oxide film can be expressed as

$$\frac{\mathrm{d}\delta_{Fe_3O_4}(t)}{\mathrm{d}t} = \frac{K_P}{2\delta_{Fe_3O_4}(t)} - \Re, \tag{1}$$

where $\delta_{Fe_3O_4}(t)$ is the oxide thickness at time t, K_P is the conventional parabolic rate constant of steel oxidation in air at the same temperature and oxygen partial pressure, i.e. $\delta(t)^2[\mathrm{air}] = K_P t$, and $\Re$ is the corrosion rate due to the flowing LBE. According to the kinetic corrosion model [30], $\Re$ depends on the global operating conditions. With oxygen control, $\Re$ is much smaller than the oxidation rate in the first thousand hours, in the present calculation, $\Re$ is neglected.

The total oxide film thickness is

$$\delta = 1.91\delta_{Fe_3O_4}. \tag{2}$$

The factor 1.91 is obtained based on the assumption that the ratio of the outer layer to the inner layer is 1:1.1 (this ratio is obtained by taking the densities of steel and magnetite as 7.90 and 5.16 g/cm^3).

According to Wagner's theory, the constant K_P can be calculated as [31]

$$K_P = \frac{4}{3}\int_{P^I_{O_2}}^{P^{II}_{O_2}} f^{-1}D^* \,\mathrm{d}\ln P_{O_2}, \tag{3}$$

where $D^*[\mathrm{m}^2/\mathrm{s}]$ is the tracer diffusion coefficient of iron in magnetite layer, f is the correlation factor for the diffusion mechanism. The value of f is approximately 0.5 when mechanism involving vacancy mechanism and in the range 0.4–1 for a mechanism involving interstitials [31]. In the present calculation, it is chosen $f = 0.5$. P_{O_2} is the oxygen partial pressure, $P^{II}_{O_2}$ is the value at the LBE/oxide interface and $P^{I}_{O_2}$ is the value at the outer/inner layer interface.

In the range of 900–1400 °C, an expression of the tracer diffusion coefficient was given as [32]

$$D^*_{Fe}[\mathrm{m}^2/\mathrm{s}] = 4\times10^{-15}\exp[1.45(\mathrm{eV})/kT]P^{2/3}_{O_2} + 8\times10^{3}\exp[-6.37(\mathrm{eV})/kT]P^{-2/3}_{O_2}, \tag{4}$$

where k is the Boltzmann constant. Comparison between the calculation based on Eq. (4) and experimental results at 500 °C [33] indicates that Eq. (4) is valid at 500 °C.

The $P^{I}_{O_2}$ is set to the oxygen partial pressure for the steel–magnetite equilibrium, and it is calculated by

$$P^{I}_{O_2} = \frac{1}{a^{3/2}_{Fe}}\exp\left(\frac{\Delta G_{Fe_3O_4}}{2RT}\right). \tag{5}$$

The $P^{II}_{O_2}$ can be calculated as [34]

$$P^{II}_{O_2} = \frac{1}{a^{2}_{Pb}}\left(\frac{c_O}{c_{O,s}}\right)^2\exp\left(\frac{2\Delta G_{PbO}}{RT}\right), \tag{6}$$

Table 2
Comparisons between calculation and experimental results for the duplex oxide films

Steel	$P^{I}_{O_2}$ (atm)	c_O (ppm)	$P^{II}_{O_2}$ (atm)	K_P (m^2/s)	Time (h)	Oxide thickness (μm)	Experimental results		Error (%)
							Time (h)	Oxide thickness (μm)	
316 at 550 °C	1.70×10^{-27}	0.03	6.64×10^{-22}	2.29×10^{-17}	1000	17.3	1000	4–10	147
					2000	24.5	2000	16–20	36
					3000	30.0	3000	10–32	43
		0.05	1.84×10^{-21}	2.30×10^{-17}	1000	17.4			
					2000	24.6			
					3000	30.1			
D-9 at 550 °C	1.63×10^{-27}	0.03	6.64×10^{-22}	2.35×10^{-17}	1000	17.6	1000	5–20	41
					2000	24.9	2000	20–36	11
					3000	30.4	3000	12–40	17
		0.05	1.84×10^{-21}	2.36×10^{-17}	1000	17.6			
					2000	24.9			
					3000	30.5			
HT-9 at 550 °C	1.24×10^{-27}	0.03	6.64×10^{-22}	2.82×10^{-17}	1000	19.3	1000	20	3.1
					2000	27.2	2000	32–36	20
					3000	33.4	3000	12–38	34
		0.05	1.84×10^{-21}	2.83×10^{-17}	1000	19.3			
					2000	27.3			
					3000	33.4			
HT-9 at 460 °C	5.94×10^{-32}	0.03	5.08×10^{-24}	3.91×10^{-19}	1000	2.27	1000	1–8	48
					2000	3.21	2000	12–14	75
					3000	3.93	3000	14–16	73
		0.05	1.41×10^{-23}	4.34×10^{-19}	1000	2.39			
					2000	3.38			
					3000	4.14			

where ΔG is the standard free energy of oxide formation, a_{pb} is the lead activity in LBE, a_{Fe} is the activity of iron in the steel and set to equal its mole fraction. c_O is the oxygen concentration in LBE and it is in the range from 0.03 to 0.05 wppm in the present experiment. $c_{O,s}$ is the oxygen solubility in LBE. The Pb activity, the free energy and the oxygen solubility can be found in Ref. [34].

In the present experiment, duplex oxide films formed on HT-9 steel at 460 °C and on 316, D-9 and HT-9 at 550 °C. The calculation results as well as the experimental results of the oxide film thickness are given in Table 2, showing good agreement. The discrepancies between the average experimental results and the calculation results are less than 50% at 550 °C except for the case of 316 steel after 1000 h. For HT-9 at 460 °C, although the difference between the calculation results and the experimental results becomes larger in time, the calculation results are still reasonable.

The parabolic rate constant K_P, with a value around 2.3×10^{-17} m^2/s, increases with decreasing Cr content. The growth rate is ordered as the following: 316 < D-9 < HT-9 at 550 °C. Increasing the oxygen concentration from 0.03 to 0.05 ppm has little influence on the constant. The magnetite dissociation partial pressure at the inner/outer oxide interface decreases with decreasing Cr content because of the increase of the activity of iron in the steel.

Although the LBE/magnetite interfacial recession due to LBE corrosion is neglected, the calculation results employing the Wagner's theory are consistent with the experimental results. This indicates that oxidation dominates the corrosion process during the first thousands of hours. Since the oxidation rate decreases in time, the liquid metal corrosion will eventually dominate the corrosion of steels in LBE, and determine the long-term corrosion rate.

From the above calculations, it can be concluded that the corrosion rate $\Re$ has few effects on the oxide thickness for short-term operations. But it is necessary to point out that $\Re$ does have significant effects on the weight changes because the large difference between the atom weights of oxygen and iron, resulting in non-parabolic trends of the weight changes. Detailed studies of the corrosion rate effects will be reported in a separate paper [35].

4.4. Influence of flowing LBE

At 460 °C, the weights of all steels increase in time and the changes approximately follow the parabolic law. While at 550 °C, except for T-410 steel which was subject to significant slot corrosion, the characteristics of the weight changes of other steels in the first 2000 h testing period is very different from that afterwards. As discussed above, when steels are exposed to flowing LBE with oxygen control, oxidation and mass transfer corrosion of the alloying components occur simultaneously. The oxidation leads to a weight gain, while the corrosion results in a weight loss. Unlike oxidation in gaseous environments, it is expected that the weight will reach a maximum value when the weight gain due to oxidation equals the weight loss due to corrosion, after which weight gain due to oxidation is smaller than the weight loss due to corrosion.

At 550 °C, the weight gain dominates the whole process initially and it reaches a turning point at around 2000 h, then the weight turns downwards because of the mass transfer corrosion. Such a phenomenon is different from the oxide growth in which the oxidation dominates the whole process in 3000 h. At 460 °C, the initial oxidation process may not have completed in 3000 h due to the much smaller mass transfer corrosion rate and oxidation rate at the lower temperature.

In addition, the nature of the weight changes at 460 °C may actually be different from that at 550 °C in the test loop according to the kinetic corrosion model [30]. The corrosion model results indicate that corrosion occurs at the high temperature of the closed loop and the corrosion products precipitate at some other cooler legs. Therefore there may be precipitation in the test leg at lower temperature and weight loss may not exist if there is no erosion due to mechanical mechanisms.

'Slot corrosion' was found on the rod specimens. It is not clear what mechanism leads to such 'slot corrosion'. Since the 'slot corrosion' locations of the rod specimens are near the pipe wall, and the assembly of test specimens might have further distorted the rods pressing them toward the pipe wall, it is speculated that the resulting small gaps and the near-stagnant LBE decrease the oxygen supply to the steel surface, leading to poor oxidation formation and protection against liquid metal corrosion.

5. Conclusion

Except for the 'slot corrosion' phenomena observed on some samples (rod samples made of 316L and T-410), the experimental results show that at 460 °C, all US steels after 3000 h of tests appear to have satisfying performance. At 550 °C, the double-layer films can protect the materials, while the single-layer oxide films could not protect the steels against the dissolution. The rod specimens underwent significant liquid metal corrosion.

For the oxide film thickness, the calculation results based on the Wagner's theory are consistent with the experimental results, indicating that the oxide growth mechanism of steels in LBE is similar to that of steels in air and steam. The oxidation process is dominated by the outward diffusion of iron. During the first thousands of hours, the liquid metal corrosion effects on the oxide thickness can be neglected if the film is protective.

The weight changes were measured after the extraction of the test specimens. Despite the occurrence of some slot corrosion, the weigh changes approximately follow a parabolic law at 460 °C. However the characteristics of weigh changes was more complex at 550 °C. The weight increases in time in the first 2000 h and then decreases. This indicates that the initial dominant oxidation process is overtaken by corrosion after about 2000 h testing.

Up till now, the data on oxidation of steels in flowing LBE are still scarce and scattered. More corrosion testing in flowing LBE is needed to understand the oxidation process, the protectiveness of the oxide films and the long-term performance of protected steels. In particular, since the protectiveness and the stability of the oxides are likely to be closely correlated with long-term corrosion resistance, systematic short-term testing is needed to establish the optimal oxygen concentration and materials composition for the most suitable protective oxides. Promising candidates should then be tested for long durations to validate long-term performance.

Acknowledgements

The first author acknowledges the support of Transmutation Research Program (TRP) at the University of Nevada, Las Vegas.

References

[1] F. Barbier, G. Benamati, C. Fazio, A. Rusanov, J. Nucl. Mater. 295 (2001) 149.
[2] H. Glasbrenner, J. Konys, G. Mueller, A. Rusanov, J. Nucl. Mater. 296 (2001) 237.
[3] F. Balbaud-Celerier, P. Beloffre, A. Terlain, A. Rusanov, J. Phys. IV France 12 (2002) Pr8-177.
[4] C. Fazio, I. Ricapito, G. Scaddozzo, G. Benamati, J. Nucl. Mater. 318 (2003) 325.
[5] C. Fazio, G. Benamati, C. Martini, G. Palombarini, J. Nucl. Mater. 296 (2001) 243.
[6] G. Benamati, C. Fazio, H. Piankova, A. Rusanov, J. Nucl. Mater. 301 (2002) 23.
[7] G. Muller et al., J. Nucl. Mater. 301 (2002) 40.
[8] L.S. Crespo, F.J. Martin Munoz, D. Gomez Briceno, J. Nucl. Mater. 296 (2001) 273.
[9] D.G. Briceno et al., J. Nucl. Mater. 296 (2001) 265.
[10] D.G. Briceno et al., J. Nucl. Mater. 303 (2002) 137.
[11] F. Barbier, A. Rusanov, J. Nucl. Mater. 296 (2001) 231.
[12] A.E. Rusanov, A.P. Demishonkov, Results of Corrosion Tests of 316, 316L, T-410, HT-9 and D-9 Steels, Technical Report to Los Alamos National Laboratory under contract: #H12030008-35 between SSCRF IPPE (Russia) and LANL, USA, 2000.
[13] N. Li, X. He, A. Rusanov, A.P. Demishonkov, Corrosion Test of US Steels in Lead–Bismuth Eutectic (LBE) and Kinetic Modeling of Corrosion in LBE systems, Report to Los Alamos National Laboratory, LA-UR-02-2028, 2002.
[14] G.Y. Lai, High Temperature Corrosion of Engineering Alloys, ASM International, The Material Information Society, 1990, p. 21.
[15] K. Kikuchi et al., J. Nucl. Mater. 318 (2003) 348.
[16] M.R. Taylor, J.M. Calvert, D.G. Lees, D.B. Meadowcroft, Oxid. Met. 14 (1980) 499.
[17] L.S. Crespo, F.J.M. Munoz, D.G. Briceno, J. Nucl. Mater. 296 (2001) 273.
[18] R.T. Pascoe, Corrosion of Ferritic Boiler Steels in Steam, Central Electricity Research Laboratories Report, No. RD/L/N 142/72.
[19] P.C. Rowlands, J.C.P. Garrett, F. Garrett, F.G. Hicks, B.K. Lister, B. Lloyd, J.A. Twelves, in: D.R. Holmes, R.B. Hill, L.M. Wyatt (Eds.), Corrosion of Steel in CO_2, British Nuclear Energy Society, London, 1974, p. 193.
[20] A. Atkinson, Rev. Mod. Phys. 57 (1985) 437.
[21] J.D. Hodge, J. Electrochem. Soc. 125 (1978) 55c.
[22] M.G.C. Cox, V.D. Ccott, B. McEnaney, Philos. Mag. 26 (1972) 839.
[23] D.G. Lees, P.C. Rowlands, P. Humphrey, Mater. Sci. Technol. 4 (1988) 1117.
[24] P. Kofstad, High Temperature Corrosion, Elsevier, 1988, p. 206.
[25] A. Atkinson, Mater. Sci. Technol. 4 (1988) 1046.
[26] R.J. Hussey, M.J. Graham, Corros. Sci. 21 (1981) 255.
[27] C. Gleave, J.M. Calvert, D.G. lees, P.C. Rowlands, Proc. R. Soc. London Ser. A 379 (1982) 409.
[28] J.E. Castle, H.G. Masterson, Corros. Sci. 6 (1966) 93.
[29] J. Robertson, Corros. Sci. 29 (1989) 1275.
[30] J. Zhang, N. Li, J. Nucl. Mater. 321 (2003) 184.
[31] N.J. Cory, T.M. Herrington, Oxid. Met. 28 (1987) 237.
[32] R. Dieckmann, H. Schmalzried, Ber. Bunsen-Ges. 81 (1977) 344.
[33] A. Atkinson, M.L. Odwyer, T.I. Taylor, J. Mater. Sci. 18 (1983) 2371.
[34] J. Zhang, N. Li, J.S. Elson, Prog. Mater. Sci., in press.
[35] J. Zhang, N. Li, J. Nucl. Mater. 326 (2004) 201.